The Coulomb problem and Rutherford scattering using the Hamilton vector

A. González-Villanueva
Laboratorio de Sistemas Dinámicos, Departamento de Ciencias Básicas, Universidad Autónoma Metropolitana-Azcapotzalco
Apartado postal 21-726, 04000 Coyoacán, D.F., Mexico

H.N. Núñez-Yépez*
Instituto de Física "Luis Rivera Terrazas", Benemérita Universidad Autónoma de Puebla
Apartado postal J-48, 72570 Puebla, Pue., Mexico

A.L. Salas-Brito†
Departamento de Física, Facultad de Ciencias, Universidad Nacional Autónoma de México
Apartado postal 21-726, 04000 Coyoacán, D.F., Mexico

Recibido el 1 de julio de 1997; aceptado el 19 de noviembre de 1997

The motion of a particle in a Coulomb field is analyzed with the help of the conserved Hamilton vector. This affords a simple way of obtaining both the orbit in configuration space and the hodograph in velocity space. We show how to obtain the Hamilton vector, then, with its help, we get the equations of both trajectories. We next show that the trajectories of the Coulomb problem in velocity space are all circular. We also exhibit a geometric method for calculating the deflection angle in the case of scattering trajectories and then we derive the Rutherford scattering formula. We also discuss an approximate method which takes advantage of the Hamilton vector for studying scattering in a centrally perturbed Coulomb field. As an example of the use of this approach the case of an inverse cubic perturbation is discussed in some detail.

Keywords: Central Field, Hamilton vector, Rutherford formula

El movimiento de una partícula en un campo coulombiano se analiza con la ayuda del vector constante de Hamilton. Ello nos permite obtener en forma sencilla tanto la órbita en el espacio de las configuraciones como la hodógrafa en el de las velocidades. Demostramos cómo obtener el vector de Hamilton y, a continuación y con su ayuda, obtenemos la ecuación de las trayectorias mencionadas exhibiendo durante el proceso la circularidad de su hodógrafa. Desarrollamos un método geométrico que nos permite obtener el ángulo de dispersión y a partir de él, la fórmula de Rutherford para la sección eficaz de dispersión. Introducimos también una técnica aproximada para calcular la función de deflexión para interacciones coulombianas perturbadas por un término central. Para ilustrar el método estudiamos con algún detalle el caso de una perturbación inversamente proporcional al cubo de la distancia.

Descriptores: Campo central, vector de Hamilton, fórmula de Rutherford

PACS: 03.20.+i

1. Introduction

The scattering of a charged particle in a Coulomb field have been discussed in many ways; for example, using the Laplace-Runge-Lenz vector, **A** [1–4]. This approach has been used even for discussing perturbed Coulomb problems, with the help of **A** many results of classical scattering theory can be rederived in a different and elegant way. In this contribution we want to exhibit that many of such results can be calculated by using the Hamilton vector, **h** a very interesting but little known "extra" constant of motion of the Coulomb problem [5, 6]. To make clear our point, we need to discuss first a rather simple way of solving the classical Coulomb problem passing through velocity space. The method, basically due to Hamilton, takes advantage of the properties of **h** and calculates first the hodograph in order to solve the problem [6–8].

The Hamilton vector is a little known constant of motion of the classical Coulomb problem which is surprisingly easy to obtain. As is the case of **A**, the Hamilton vector is related to the hidden symmetries of the problem and can be considered as a manifestation of its superintegrability. That is, its existence can be regarded as a manifestation of the fact that in the Coulomb problem there are constants of motion in excess to the minimum number (three in the Coulomb case) assuring its integrability. Or, to express the idea in yet another way, **h** can be related to the existence of a Hamilton-Jacobi equation separable in more than one system of coordinates [4, 7, 9].

A beautiful but, nowadays, little known feature of the Coulomb problem is that all the trajectories of the problem are circular in velocity space. This makes velocity space geometrically simpler than configuration space [6, 10, 11]. Thus, as was realized by Fano and Fano [12] and by Feynman [13] a long time ago, it can be regarded as a natural arena for discussing scattering and certain geometric features on the problem. The advantages of using **h** for describing scattering come basically from its close relationship with the hodograph of the Coulomb problem, *i.e.* with its trajectory in velocity

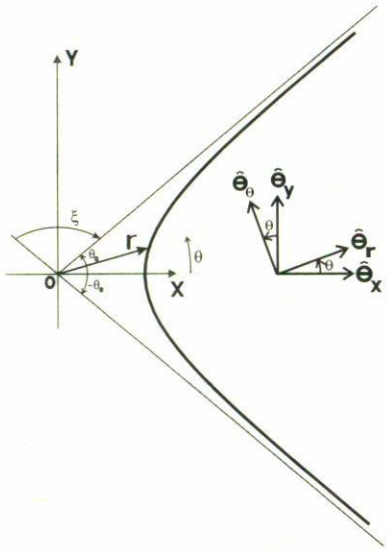

FIGURE 1. The coordinate systems used to describe the problem are illustrated. The z-axis points outside of the plane of the paper and the x-axis goes through both the center of force at the origin (marked **O**) and the pericentre of the orbit. A hyperbolic scattering trajectory is shown together with their asymptotes (the thin straight lines), $-\theta_0$ and $+\theta_0$ are, respectively, the angles that the incoming and the outgoing asymptotes make with the x-axis; ξ is the deflection angle and it is clear that $\xi/2 + \theta_0 = \pi$.

space. This happens since a classical scattering process, when there exist asymptotic states as in Coulomb's case, has mainly to do with the relationship between the asymptotic incoming and the asymptotic outgoing velocities [3].

2. The Hamilton vector and the Coulomb problem

In this section we derive the vector constant known as the Hamilton vector, **h**. We will discuss how to use it to obtain the equation of the orbit and to show that the problem's hodograph is a circle or a circular arc.

To begin with, let us consider the equation of motion of a particle in an inverse squared field fixed at the origin

$$m\frac{d^2\mathbf{r}}{dt^2} = \frac{\alpha}{r^2}\hat{\mathbf{e}}_r, \tag{1}$$

where m is the mass, $\hat{\mathbf{e}}_r$ the unit vector in the radial direction, $\mathbf{r}$ the position vector of the particle and α is a constant characterizing the intensity of the interaction—for Coulomb interaction we should have $\alpha = qq'/4\pi\epsilon_0$. The angular momentum, $\mathbf{L} = m\mathbf{r}\times\mathbf{v} = mr^2\dot{\theta}\hat{\mathbf{e}}_\mathbf{z} = L\hat{\mathbf{e}}_\mathbf{z}$ and the energy E are constants of motion as in every central field problem. We have selected the x-y plane as the orbital plane, $\dot{\theta}$ is the particle's angular velocity and we use a cylindrical coordinate system in which the polar axis coincides with the x-axis and passes through both the center of force and the point on the orbit closer to it, as Fig. 1 illustrates.

Using the elementary results $\dot{\hat{\mathbf{e}}}_\theta = -\dot{\theta}\hat{\mathbf{e}}_r$, $\dot{\theta} = L/mr^2$ and angular momentum conservation in Eq. (1), where $\hat{\mathbf{e}}_\theta$ is the unit vector orthogonal to $\hat{\mathbf{e}}_r$ in the direction of increasing θ, we get

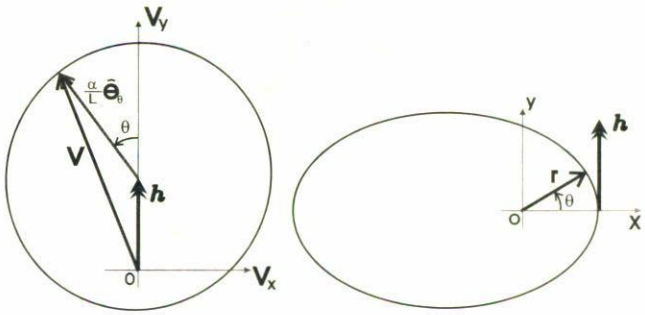

FIGURE 2. The Coulomb problem hodograph is always a circle centered at **h** and with radius $|\alpha|/L$. In the case shown here the origin of coordinates in velocity space (v-origin) is inside the hodograph, *i.e.* we have $h < |\alpha|/L$ and then $E_c < E < 0$. We have chosen **h** and hence the velocity at pericentre $\mathbf{v}_p$, pointing in the y-direction. This corresponds to an elliptic orbit in configuration space oriented with its major axis along the x-axis as shown. The particular case in which the v-origin coincides with the hodograph centre (*i.e.* when $\mathbf{h} = 0$, $E = E_c \equiv -m\alpha^2/2L^2$) corresponds to a circular orbit in configuration space.

$$m\frac{d\mathbf{v}}{dt} = -\frac{m\,\alpha}{L}\frac{d\hat{\mathbf{e}}_\theta}{dt}, \tag{2}$$

it is now very easy to derive a new constant of motion for the Coulomb problem [6, 14, 15], the so-called Hamilton vector

$$\mathbf{h} = \mathbf{v} + \frac{\alpha}{L}\hat{\mathbf{e}}_\theta. \tag{3}$$

It is worth noting that $\mathbf{h}\cdot\mathbf{L} = 0$ and that, in configuration space, **h** points along the semilatus rectum of the orbit *i.e.* it is necessarily parallel to the velocity at pericentre [see Eq. (6) below] [6]. In the coordinate system illustrated in Fig. 1, the Hamilton vector points along the y axis: $\mathbf{h} = h\,\hat{\mathbf{e}}_y$. We can now express the velocity as the sum of the constant vector **h** plus a rotating vector with constant magnitude:

$$\mathbf{v} = \mathbf{h} - \hat{\mathbf{e}}_\theta\,\frac{\alpha}{L}; \tag{4}$$

the rotating component of the velocity is always perpendicular to $\mathbf{r}$. This equation means that any $L \neq 0$ trajectory in velocity space is a circle of radius $|\alpha|/L$ centered at **h**. This is illustrated in Figs. 2, 3, and 4. Curiously, as expressed in a recent book [11], "this startling fact—the circularity of the hodograph—is unknown to most physicist" despite its many implications in both the physics and the geometry of the Coulomb problem [10, 11, 16].

The Hamilton vector **h** contains most of the dynamic information on the motion [5, 16], for example, it is elementary to obtain the polar components of the velocity and their dependence on θ,

$$\begin{aligned} v_r(\theta) &= \mathbf{v}\cdot\hat{\mathbf{e}}_r = h\sin\theta, \\ v_\theta(\theta) &= \mathbf{v}\cdot\hat{\mathbf{e}}_\theta = h\cos\theta - \frac{\alpha}{L}, \end{aligned} \tag{5}$$

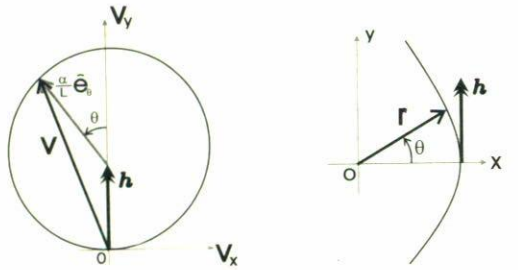

FIGURE 3. If the v-origin sits on the hodograph, *i.e.* if $h = |\alpha|/L$, $E = 0$ and $\epsilon = 1$, the configuration space orbit is the parabola shown. In this case the v-origin represents the asymptotic velocities at infinity: $\mathbf{v}_{+\infty} = \mathbf{v}_{-\infty} = 0$.

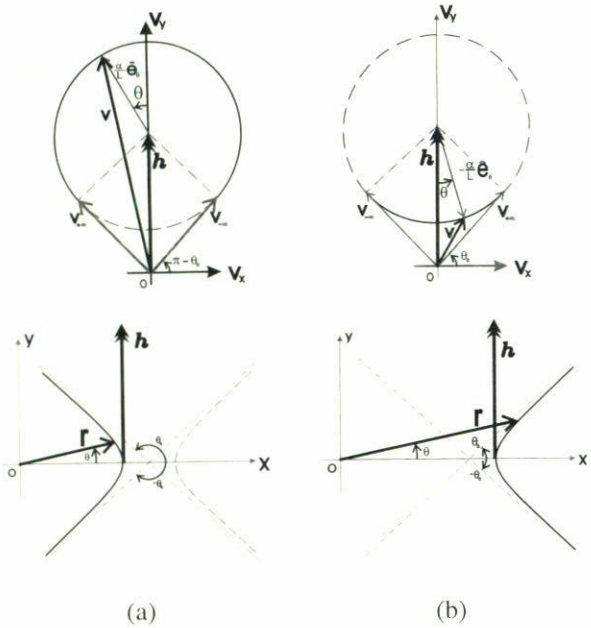

(a) (b)

FIGURE 4. If the v-origin is outside the hodograph, *i.e.* if $h > |\alpha|/L$, $E > 0$ and the whole hodograph is just the dark circular arc bounded between the angles $-\theta_0$ and $+\theta_0$, where $\cos\theta_0 = 1/\epsilon$. Notice that the whole circle corresponds to the two branches of the hyperbola. The two possible cases are shown: (a) The attractive case $\alpha < 0$, where the hodograph is concave towards the origin. The asymptotic velocity vector $\mathbf{v}_{-\infty}$ makes an angle $-\theta_0$ (or, as shown and equivalently, an angle $\pi - \theta_0$) with the x-axis. In this case the centre of force sits at the internal focus of the configuration space hyperbola. The light dashed curve shown in Fig. 4a (and in 4b) corresponds to the branch of the hyperbola not actually traversed. (b) The repulsive case $\alpha > 0$, where the hodograph is convex towards the origin. The asymptotic velocity vector $\mathbf{v}_{+\infty}$ makes an angle $+\theta_0$ (or, equivalently, an angle $\theta_0 - \pi$) with the x-axis, as shown. The center of force is located at the external focus of the hyperbola. This figure is sort of the reverse of Fig. 4a.

where v_r and v_θ are, respectively, the radial and azimuthal components of the velocity and h is the magnitude of $\mathbf{h}$. These are the parametric equations of a circle in velocity space; so, as we claimed before, the hodograph is a circle or circular arc—depending on the range allowed for θ.

From Eq. (5) and the expression $v_\theta = r\dot{\theta}$, the equation of the orbit follows immediately:

$$r = \frac{p}{\epsilon\cos\theta - \operatorname{sgn}\alpha}, \tag{6}$$

where sgn stands for the signum function ($\operatorname{sgn} x = 1$ if $x > 0$ or $\operatorname{sgn} x = -1$ if $x < 0$), we have defined $p \equiv L^2/m|\alpha|$ and $\epsilon \equiv Lh/|\alpha|$. Equation (6) is obviously the polar equation of a conic section with eccentricity ϵ and semilatus rectum p; to completely characterize the conic section we have to take into account the algebraic sign of α. It is worth pointing out the simplicity of the process for getting the general form of the orbit with the help of $\mathbf{h}$.

Notice that expression (5) implies that the velocity at pericentre, like $\mathbf{h}$, points in the y-direction. Although it is implicit in the definition of ϵ, it can be useful to emphasize that the magnitude of $\mathbf{h}$ can be written as

$$h = \epsilon\frac{|\alpha|}{L}. \tag{7}$$

On the other hand, notice that the energy of the motion can be expressed in terms of h in the alternative forms

$$E = \frac{m}{2}\left(h^2 - \frac{\alpha^2}{L^2}\right) = \frac{m\alpha^2}{2L^2}(\epsilon^2 - 1). \tag{8}$$

Furthermore, the famous Laplace-Runge-Lenz vector [3] can be easily obtained as

$$\mathbf{A} = \mathbf{h}\times\mathbf{L} = \mathbf{v}\times\mathbf{L} + \alpha\,\hat{\mathbf{e}}_r; \tag{9}$$

the constancy of $\mathbf{A}$ follows as a simple consequence of the constancy of $\mathbf{h}$ and of $\mathbf{L}$.

We can now show using Eqs. (4), (6) and (8), that the type of motion changes according to where the origin of coordinates in velocity space is located in relation to the hodograph [6, 10]:

a) If the hodograph centre coincides with the origin of coordinates in velocity space, *i.e.* if $h = 0$, the configuration space orbit is also circular and the hodograph is the whole circle. In this case, as follows from (8), $E = E_c \equiv -m\alpha^2/2L^2$. If the origin of coordinates is inside the hodograph but does not sit on its center, *i.e.* if $h < |\alpha|/L$, we must have $E_c < E < 0$, the hodograph is also the whole circle and the configuration space orbit is an ellipse. The former case is a particular instance of the later. See Fig. 2.

b) If the origin of coordinates in velocity space sits on the hodograph, *i.e.* if $h = |\alpha|/L$, there is a point with asymptotically vanishing velocity, we have $E = 0$, and the hodograph is again the whole circle. In this case the orbit in configuration space is a parabola. This is illustrated in Fig. 3.

c) If the origin of coordinates in velocity space is outside the hodograph, *i.e.* if $h > |\alpha|/L$, we have $E > 0$, the hodograph is not the whole circle but just a circular arc—the arc's limiting angles are found solving the equation $\cos\theta_0 = 1/\epsilon$; θ_0 is the incident angle (Fig. 1). The configuration space orbit is hyperbolic in this case. Another fact worth of mentioning here is the compactification achieved by introducing

the hodograph: the whole infinity trajectory in configuration space is mapped to the finite circular arc of the hodograph. Fig. 4a illustrates the case $\alpha < 0$ whereas Fig. 4b illustrates the case $\alpha > 0$.

In the rest of the article we assume that the configuration space orbit is a hyperbola as corresponds to a scattering trajectory. We also assume that the scattering occurs in a repulsive ($\alpha > 0$) Coulomb field—according to (6), only hyperbolas are allowed as solutions in such a case. Notice also that, as the denominator in (6) must be non-negative, if $\epsilon > 1$ the only orbits allowed are necesarily confined between the non-null angles $-\theta_0$ and $+\theta_0$. These angles are the directions of the asymptotes of the hyperbola, or, respectively, of the incoming, $\mathbf{v}_{-\infty}$, and outgoing, $\mathbf{v}_{+\infty}$, velocities. In these conditions, the external focus of the hyperbola coincides with the center of force as shown in Fig. 4b.

We have illustrated how the unperturbed Coulomb problem can be solved with the help of $\mathbf{h}$. To conclude the section, let us point out that although we have found that the number of constants in the problem is 7 (or even 10, in we include the components of $\mathbf{A}$) namely, the energy, plus the three components of $\mathbf{L}$, plus the three components of $\mathbf{h}$, only 5 constants out of the original 7 can be independent [9], otherwise the system would be overdetermined [4]. The existence of 5 independent constants of motion is described by saying that the problem is superintegrable [7, 16].

3. Scattering in a Coulomb field and the Rutherford formula

In this section we show how to use $\mathbf{h}$ and the hodograph to derive the Rutherford scattering formula. Therefore, in this section and in the rest of the article, we assume $E > 0$ and, hence, that all orbits are hyperbolic. For convenience we also assume that $\alpha > 0$, although this is not strictly necessary since the discussion is also applicable, with minor changes, to the case $\alpha < 0$.

In Fig. 5 (which is basically the hodograph shown in Fig. 4b) the quantities pertaining to scattering are clearly depicted. We thus infer that, using $\mathbf{h}$ and the hodograph, it should be very easy to compute the deflection angle ξ, and hence that the Rutherford formula for scattering in a Coulomb field must also follow using the standard methods. In the diagram (see also Fig. 1) it is clear that θ_0 and ξ are related by $\theta_0 + \xi/2 = \pi/2$. For obtaining the appropriate relations between such quantities, let us note that, as the Hamilton vector suffers no changes during the motion, for the whole scattering trajectory (as for any part of it) we ought to have

$$\Delta\mathbf{h} = \Delta\mathbf{v}_\infty + \frac{\alpha}{L}\Delta\hat{\mathbf{e}}_\theta = 0, \tag{10}$$

where the change $\Delta\hat{\mathbf{e}}_\theta$ is evaluated by substracting the incoming from the outgoing angular unit vector, as illustrated

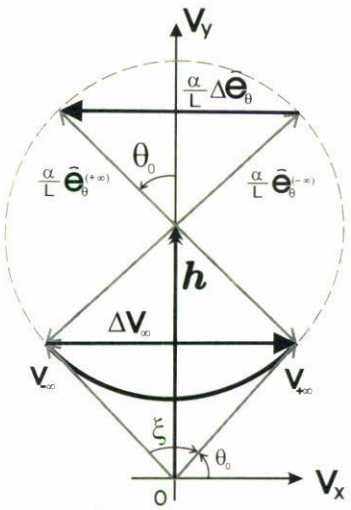

FIGURE 5. The Coulomb problem hodograph in the repulsive case (compare with Fig. 4b). It is easy to see that the incident and deflection angles are related by $\theta_0 + \xi/2 = \pi/2$. It is also easy to see from simple geometry that $\Delta\mathbf{v}_\infty = 2v_\infty \sin(\xi/2)\hat{\mathbf{e}}_x$ and that $(\alpha/L)\,\Delta\hat{\mathbf{e}}_\theta = -(2\alpha/L)\sin\theta_0\,\hat{\mathbf{e}}_x$.

in Fig. 5. As a result of the scattering, the velocity changes in

$$\Delta\mathbf{v}_\infty = \mathbf{v}_{+\infty} - \mathbf{v}_{-\infty} = 2v_\infty \sin\frac{\xi}{2}\hat{\mathbf{e}}_x, \tag{11}$$

and the unit angular vector changes in

$$\Delta\hat{\mathbf{e}}_\theta = \hat{\mathbf{e}}_\theta(+\infty) - \hat{\mathbf{e}}_\theta(-\infty) = -2\sin\theta_0\hat{\mathbf{e}}_x, \tag{12}$$

during the whole process. Equations (11) and (12) follow, using simple geometry, from Fig. 5. Moreover, since $\xi/2 + \theta_0 = \pi/2$ we have $\cos(\xi/2) = \sin\theta_0$ and, by plugging results (11) and (12) into Eq. (10), we get

$$\Delta\mathbf{h} = 2\left(v_\infty \sin\frac{\xi}{2} - \frac{\alpha}{L}\cos\frac{\xi}{2}\right)\hat{\mathbf{e}}_x = 0. \tag{13}$$

Thence, we see that L and the incoming speed, v_∞, are related by the so-called Rutherford relation

$$L = \frac{\alpha}{v_\infty}\cot\frac{\xi}{2}. \tag{14}$$

From this expression, it is immediate to get, in the standard way, the differential scattering cross section in a Coulomb field [3]

$$\frac{d\sigma}{d\Omega} = \frac{1}{m^2v_\infty^2}\left|\frac{L}{\sin\xi}\frac{dL}{d\xi}\right| = \left(\frac{\alpha}{2mv_\infty^2}\right)^2\frac{1}{\sin^4\xi/2}. \tag{15}$$

This is Rutherford's differential scattering cross section, which happens to be independent of the sign of α, that is, in (15) it does not matter whether the interaction is repulsive or attractive.

4. Scattering in a perturbed Coulomb field.

In this section we illustrate the value of the Hamilton vector for describing scattering even in a perturbed but still central Coulomb problem.

If the perturbing term has the form $\mathbf{f}(r) = f(r)\hat{\mathbf{e}}_r$, the equation of motion becomes

$$m\frac{d^2\mathbf{r}}{dt^2} = \frac{\alpha}{r^2}\hat{\mathbf{e}}_r + f(r)\hat{\mathbf{e}}_r. \tag{16}$$

Despite the fact that in this case is no longer conserved, the Hamilton vector is still useful for doing certain scattering calculations. In this section we discuss the problem following the ideas presented in Ref. 1, but using $\mathbf{h}$ instead of $\mathbf{A}$.

When a perturbation is present the equation of motion of the Hamilton vector [13] follows from (3) and (16)

$$\frac{d\mathbf{h}}{dt} = \frac{f(r)}{m}\hat{\mathbf{e}}_r. \tag{17}$$

It is useful to transform (17) to a differential equation in θ, first, it is obvious that

$$\frac{d\mathbf{h}}{dt} = \frac{d\mathbf{h}}{d\theta}\dot{\theta}, \tag{18}$$

next, using the conservation of L, from this follows that

$$\frac{d\mathbf{h}}{d\theta} = \frac{r^2 f(r)}{L}\hat{\mathbf{e}}_r. \tag{19}$$

Although in principle Eq. (17) can be integrated along the scattering trajectory to get the change in $\mathbf{h}$, this is of no use (unless we do it numerically) since we do not know the trajectory from the start. However, Eq. (19) can be used to get a first order approximation to the trajectory valid when the perturbation $f(r)$ might be regarded as small [2, 14], *i.e.* if $|f(r)| \ll \alpha/r^2$ in the range of r-values important for the scattering process. An explicit illustration of the use of the criterion is given in the next section.

Let us assume the above criterion is met; so, let us integrate Eq. (19) along the *unperturbed* scattering trajectory, to get

$$\begin{aligned}\delta\mathbf{h} &= \frac{\hat{\mathbf{e}}_x}{L}\int_{-\theta_0}^{\theta_0} r^2 f(r)\cos\theta d\theta + \frac{\hat{\mathbf{e}}_y}{L}\int_{-\theta_0}^{\theta_0} r^2 f(r)\sin\theta d\theta \\ &= \frac{\hat{\mathbf{e}}_x}{L}\int_{-\theta_0}^{\theta_0} r^2 f(r)\cos\theta d\theta.\end{aligned} \tag{20}$$

Since $\mathbf{h} = h\,\hat{\mathbf{e}}_y$ then $\mathbf{h}\cdot\delta\mathbf{h} = 0$; in this way, we have explicitly got that the change in $\mathbf{h}$ is orthogonal to itself. As follows from $v_\infty^2 = h^2 - \alpha^2/L^2$, this result also implies that $\mathbf{v}_\infty \cdot \delta\mathbf{v}_\infty = 0$. That is, in this approximation, although the asymptotic velocity changes, it only rotates but never modifies its length. Thus we can say that the perturbation produces a rotation of $\mathbf{h}$ in the scattering plane by an angle given by $\tan\delta\xi = \delta h/h$, but, in the approximation we are working with, $\tan\delta\xi \simeq \delta\xi$, since we assume $\delta\xi \ll 1$. That is, as a first approximation, we may regard $\mathbf{h}$ as just undergoing a clockwise rotation—counterclockwise, in the case of an attractive perturbation—by an angle $\delta h/h$. But this can be easily interpreted as a rotation of the incoming and outgoing asymptotes by this angle. Thus the whole proces may be described as a combination of two auxiliary trajectories: an incoming auxiliary Coulomb-like trajectory plus another auxiliary Coulomb-like outgoing trajectory which have to appropriately "interpolated" in the middle to construct the approximate trajectory of the perturbed problem. All of this is illustrated in Fig. 6 with both configuration space orbits and hodographs.

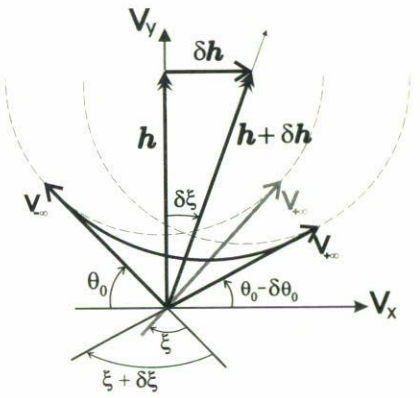

(a)

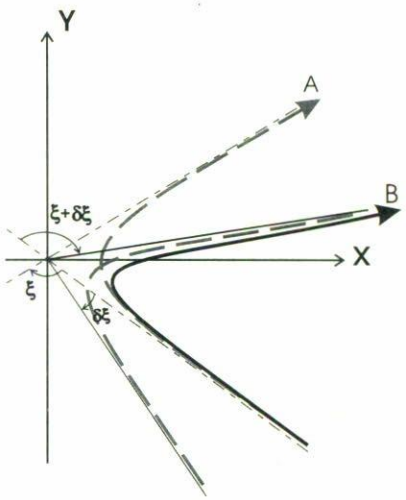

(b)

FIGURE 6. Rotation of a scattering trajectory under a conservative central perturbation. The perturbing force is assumed repulsive. For the sake of clarity, the results of the perturbation have been exagerated. (a) Schematic representation of the effect of a central repulsive ($\beta > 0$) perturbation on the hodograph. The two, one incoming and the other outgoing, auxiliary Coulomb like hodographs are shown as light dashed circles shifted to each other by $\delta\mathbf{h}$. The actual hodograph of the perturbed problem is the dark curve shown interpolating between the auxiliary hodographs. (b) The configuration space orbits corresponding to the hodographs illustrated in Fig. 4a. The auxiliary trajectories are shown as dashed light curves. **A** and **B** mark, respectively, the auxiliary incoming and the auxiliary outgoing trajectories. The solid dark curve corresponds to the actual perturbed orbit. The straight lines shown are the asymptotes of the auxiliary trajectories.

All the results mentioned above are just an approximation to the process if the perturbing force $f(r)$ is reasonably small. It is interesting to note that the approximation treated here can even deal with the strong but short range nuclear forces, we only need to guarantee a distant collision process for, in such a case, even the nuclear interaction may be considered as a perturbation to the Coulomb force [2]. Under such conditions and if the perturbation is repulsive, *i.e.* if $f(r) > 0$, we have argued that the deflection angle increases by $\delta\xi$ and so it becomes

$$\begin{aligned}\xi &= \xi_c + \delta\xi \\ &= 2\,\mathrm{arccot}\left(\frac{Lv_\infty}{\alpha}\right) + \frac{1}{Lh}\int_{-\theta_0}^{\theta_0} r^2 f(r)\cos\theta d\theta; \end{aligned} \quad (21)$$

where ξ_c refers to the deflection angle in the unperturbed Coulomb case, which can be obtained from Eq. (14). This expression can be used as the starting point for deriving first-order approximations to the differential cross section for some scattering problems. To illustrate the method, in the next section we discuss scattering in a Coulomb field perturbed by a $1/r^3$ interaction.

5. An example: scattering in a r^{-3}-perturbed Coulomb field.

To illustrate what we have been discussing, let us select the explicit form $f(r) = \beta/r^3$, where β is a constant, for the perturbation. This term makes the perturbed problem exactly solvable [17], but even this is not really a complete advantage because there is no way of inverting the solution for getting explicit expressions for L as function of ξ and thus neither for calculating exactly the differential scattering cross section. This kind of trouble with a solvable example just contributes to illustrate the usefulness of the approximate method. On the other hand, the perturbation selected allows the direct comparison of the approximate expression for ξ, calculated with the method of the previous section, with the exact result calculated in the Appendix.

With the explicit expression for the perturbation and, employing Eq. (6) as the Coulomb solution $r(\theta)$, we get for the rotation angle

$$\begin{aligned}\delta\xi &= \frac{1}{hL}\int_{-\theta_0}^{\theta_0}\frac{\beta}{r}\cos\theta\, d\theta \\ &= \frac{\beta}{hLp}\int_{-\theta_0}^{\theta_0}(\epsilon\cos\theta - 1)\cos\theta\, d\theta, \end{aligned} \quad (22)$$

or, effecting the elementary integration, we obtain

$$\delta\xi = \frac{\beta}{hpL}(\epsilon\theta_0 - \sin\theta_0), \quad (23)$$

this result shows that the deflection angle increases when $\beta > 0$ and that the outgoing angle θ_0 diminishes by $\delta\theta_0 = -\delta\xi/2$. The change in the deflection angle (23) can be also expressed as

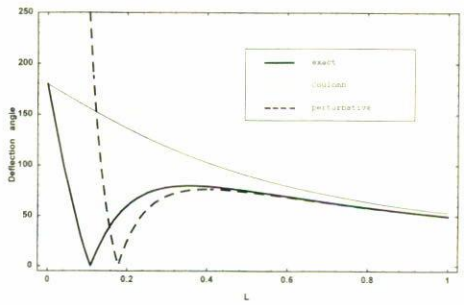

FIGURE 7. Absolute value of the deflection angle in a $1/r^3$-perturbed Coulomb field calculated exactly (continuous dark line) and in the first-order approximation discussed in the text (dashed dark line). The absolute value of the deflection angle in the unperturbed Coulomb case (continuous light curve) is also shown for comparison. The angles are in degrees. The values used for the parameters of the problem were $E = 2$, $\alpha = 1$, $m = 1$, and $\beta = 0.025$ in arbitrary units, L is also in arbitrary units.

$$\begin{aligned}\delta\xi &= \frac{m\beta}{2L^2}(\pi - \xi_c - \sin\xi_c) \\ &= E\frac{\beta}{\alpha^2}\frac{(\pi - \xi_c - \sin\xi_c)}{\cot^2\xi_c/2}, \end{aligned} \quad (24)$$

where we are assuming that L and E take the same values as in the unperturbed Coulomb case—as it is easy to realize, this is always possible without losing any generality. Thence, according to Eq. (20), the deflection angle in the perturbed case can be approximated as

$$\xi = \xi_c + E\frac{\beta}{\alpha^2}\frac{(\pi - \xi_c - \sin\xi_c)}{\cot^2\xi_c/2}. \quad (25)$$

A comparison of this approximation against the exact result is shown in Fig. 7, where we plot, as it is usually done since an experiment just detects this, the absolute values of the approximate deflection angle Eq. (25), the absolute value of the exact deflection angle [calculated in the Appendix, see Eq. (A3)] and, for purposes of comparison, the deflection angle for the unperturbed Coulomb case [2]. As you can see in the figure, the approximation is fairly good save at low values of L (say, for $L < 0.35$), that is, only if the trajectory comes close to the center of force, but even so, it reproduces the trend in the behavior of ξ.

Now, to compute the changes in the Rutherford differential scattering cross section produced by the presence of the perturbation we only need to apply the standard formula given in (15). However, as expression (25) is rather difficult to invert for getting L as a function of ξ—since ξ_c also depends on L—we use another approach which takes advantage of the smallness of $\delta\xi$. To this end, let us write for the perturbed differential cross section

$$\frac{d\sigma}{d\Omega} = \left(\frac{\alpha}{2mv_\infty^2}\right)^2 \frac{1}{\sin^4(\xi_c + \delta\xi)/2}; \quad (26)$$

the effect of the perturbation can be estimated by just power expanding (26) and taking the absolute value of the result [2]

$$\frac{d\sigma}{d\Omega} = \left(\frac{\alpha}{2mv_\infty^2}\right)^2 \frac{1}{\sin^4 \xi/2} |1 - 2\,\delta\xi\, \cot \xi/2| \qquad (27)$$

where, at it is no longer important, we have removed the subscript c and, as before, we assumed that there is no change in the angular momentum. This expression, which may be assumed correct to first order in $\delta\xi$, can be regarded as the differential scattering cross section in a Coulomb field perturbed by a r^{-3} field. Notice that, as it was to be expected, the perturbation losses effectivity on increasing the projectile's angular momentum [compare with the first of Eqs. (24) and take a look at Fig. 7]. That is, the approximation is better the farther from the field travels the projectile.

Acknowledgments

The work has been partially supported by CONACyT (grant 1343P-E9607). The Fundación Ricardo J. Zevada has provided the funds for adquiring the software in which the figures were drawn. We also want to thank K. Hryoltiy and G. Candelita for their very useful comments. This paper is dedicated to the memory of our beloved friends F. Ek, Q. Tomi, M. Gluckhen, M. Mizton, M. Mina, B. Minina, and M. Motita.

Appendix

The only purpose of the appendix is to derive the exact formula for the deflection angle in the Coulomb problem perturbed by an inverse cubic term. The effective potential energy for the perturbed problem reads

$$U_{eff}(r) = \frac{\alpha}{r} + \frac{\beta}{2r^2} + \frac{L^2}{2mr^2}, \qquad (A1)$$

therefore, according to Eq. (18.2) in Ref. 2, the deflection angle can be calculated as

$$\xi = \pi - 2\int_{r_p}^{\infty} \frac{L/r^2 dr}{\sqrt{2m(E - U_{eff}(r))}}; \qquad (A2)$$

where $r_p = \alpha(1 + \sqrt{1 + 2E(L^2 + \beta m)/m\alpha^2})/2E$ is the distance to pericentre in the perturbed problem. Effecting the integral in (A2) we get

$$\xi = \pi - 2\arcsin\left[\frac{m\alpha^2}{\sqrt{1 + 2E(L^2 + m\beta)}}\right] - 2\arcsin\left[\frac{2E(L^2 + m\beta)}{m\alpha^2 + 2E(L^2 + m\beta) + \sqrt{m\alpha^2(m\alpha^2 + 2E(L^2 + m\beta))}} + \frac{m\alpha^2}{m\alpha^2 + 2E(L^2 + m\beta)}\right], \qquad (A3)$$

where $E = mv_\infty^2/2$. This is the exact expression for the deflection angle in the perturbed Coulomb problem. In the case $\beta = 0$, Eq. (A3) can be shown to reduce to the Coulomb expression. In Fig. 7 we compare the exact formula (A3) with the first order expression for ξ given in Eq. (25), we also plot there the deflection angle for the unperturbed Coulomb problem.

*. On sabbatical leave from Departamento de Física, UAM-Iztapalapa

†. On sabbatical leave from Departamento de Ciencias Básicas, UAM-Azcapotzalco

1. L. Basano and A. Bianchi, *Am.J. Phys.* **48** (1980) 400.
2. C.E. Aguiar and M.F. Barroso, *Am.J. Phys.* **64** (1996) 10042.
3. L. Landau and E.M. Lifshitz, *Mechanics*, (Pergamon, Oxford, 1976), Chap. IV.
4. R.P. Martínez-y-Romero, H.N. Núñez-Yépez and A.L. Salas-Brito, *Eur.J. Phys.* **13** (1992) 26.
5. H. Goldstein, *Am.J. Phys.* **44** (1976) 1123.
6. A. González-Villanueva, H.N. Núñez-Yépez, and A.L. Salas-Brito, *Eur. J. Phys.* **17** (1996) 168.
7. R.P. Martínez-y-Romero, H.N. Núñez-Yépez, and A. L. Salas-Brito, *Eur. J. Phys.* **14** (1993) 71.
8. O. Campuzano-Cardona, H.N. Núñez-Yépez, A.L. Salas- Brito, and G.I. Sánchez-Ortiz, *Eur. J. Phys.* **16** (1995) 220.
9. N.W. Evans, *Phys. Rev. A* **41** (1990) 5666.
10. J. Milnor, *Am. Math. Monthly* **90** (1983) 353.
11. M.C. Gutzwiller, *Chaos in Classical and Quantum Mechanics*, (Springer, New York, 1990), p. 180.
12. U. Fano and L. Fano, *Basic Physics of Atoms and Molecules*, (Wiley, New York, 1958) Appendix III.
13. D.L. Goodstein and J.R. Goodstein, *Feynman's lost lecture, the motion of planets around the sun*, (Norton, New York, 1996).
14. J. Sivardière, *Eur. J. Phys.* **13** (1992) 64.
15. D. Moreno, *Gravitación Newtoniana*, (FCUNAM, México City, 1990).
16. A.L. Salas-Brito, H.N. Núñez-Yépez, and R.P. Martínez-y-Romero, *Intl. J. Mod. Phys. A* **12** (1997) 271.
17. E.T. Whittaker, *A treatise on the analytical dynamics of particles and rigid bodies*, 4th edition, (Cambridge Univ. Press, Cambridge, 1989), §46, p. 83.